Population genomics of *Plasmodium ovale* species in sub-Saharan Africa

Kelly Carey-Ewend[1], Zachary R. Popkin-Hall[2], Alfred Simkin[3], Meredith Muller[2], Chris Hennelly[2], Wenqiao He[2], Kara A. Moser[2], Claudia Gaither[2], Karamoko Niaré[3], Farhang Aghakanian[2], Sindew Feleke[4], Bokretsion G. Brhane[4], Fernandine Phanzu[5], Kashamuka Mwandagalirwa[6], Ozkan Aydemir[7], Colin J. Sutherland[8], Deus S. Ishengoma[9,10], Innocent M. Ali[11], Billy Ngasala[12], Albert Kalonji[5], Antoinette Tshefu[6], Jonathan B. Parr[2,13,14], Jeffrey A. Bailey[3], Jonathan J. Juliano[1,2,13,14,#], Jessica T. Lin[2,13,15,#]

[1]: Department of Epidemiology, Gillings School of Global Public Health, University of North Carolina, Chapel Hill, NC, USA
[2]: Institute for Global Health and Infectious Diseases, University of North Carolina, Chapel Hill, NC, USA
[3]: Department of Pathology and Laboratory Medicine, Brown University, Providence, RI, USA
[4]: Ethiopian Public Health Institute, Addis Ababa, Ethiopia
[5]: SANRU Asbl, Kinshasa, DRC
[6]: Kinshasa School of Public Health, Kinshasa, DRC
[7]: Program in Molecular Medicine, Chan Medical School, University of Massachusetts, Worcester, MA, USA
[8]: London School of Hygiene and Tropical Medicine, London, UK
[9]: National Institute for Medical Research (NIMR), Dar es Salaam, Tanzania
[10]: Department of Biochemistry, Kampala International University in Tanzania, Dar es Salaam, Tanzania
[11]: Department of Biochemistry, Faculty of Science, University of Dschang, Cameroon
[12]: Muhimbili University of Health and Allied Sciences, Dar es Salaam, Tanzania
[13]: Division of Infectious Diseases, University of North Carolina School of Medicine, University of North Carolina, Chapel Hill, NC, USA
[14]: Curriculum in Genetics and Molecular Biology, University of North Carolina School of Medicine, University of North Carolina, Chapel Hill, NC, USA
[15]: Department of Microbiology and Immunology, University of North Carolina School of Medicine, University of North Carolina, Chapel Hill, NC, USA

#: Co-senior authors

Abstract

Plasmodium ovale curtisi (*Poc)* and *Plasmodium ovale wallikeri* (*Pow*) are relapsing malaria parasites endemic to Africa and Asia that were previously thought to represent a single species. Amid increasing detection of ovale malaria in sub-Saharan Africa, we performed a population genomic study of both species across the continent. We conducted whole-genome sequencing of 25 isolates from Central and East Africa and analyzed them alongside 20 previously published African genomes. Isolates were predominantly monoclonal (43/45), with their genetic similarity aligning with geography. *Pow* showed lower average nucleotide diversity (1.8×10^{-4}) across the genome compared to *Poc* (3.0×10^{-4}) ($p < 0.0001$). Signatures of selective sweeps involving the dihydrofolate reductase gene were found in both species, as were signs of balancing selection at the merozoite surface protein 1 gene. Differences in the nucleotide diversity of *Poc* and *Pow* may reflect unique demographic history, even as similar selective forces facilitate their resilience to malaria control interventions.

Introduction

Parasites in the genus *Plasmodium* were responsible for an estimated 249 million cases of malaria and 608,000 deaths in 2022.[1] Ninety-four percent of these cases occurred in the World Health Organization Africa Region, where control efforts have primarily focused on the predominant species, *P. falciparum* (*Pf*).[2] Yet these case counts likely underrepresent the burden of non-falciparum species, which may be rising in prevalence even where control efforts have successfully reduced *P. falciparum* transmission.[3–5] Over the last few decades, genomic studies of *P. falciparum* have enabled monitoring of drug resistance markers,[6] facilitated the identification of promising vaccine candidates,[7] uncovered the structure of parasite populations,[8] and identified evolutionary forces shaping their demography.[9,10] Much less is known about non-falciparum species, especially their comparative evolutionary history and susceptibility to malaria control interventions focused on *P. falciparum*.

Plasmodium ovale was first identified as a separate malaria species in 1922 based on the appearance of oval-shaped erythrocytes that contained non-ring parasite forms.[11] Hallmarks of this parasite species are its restriction to younger red cells and therefore propensity to cause low-density infections, as well as relapses from liver hypnozoites, similar to *P. vivax* and *P. cynomologi*. The species often causes co-infection alongside *P. falciparum* which, along with its low parasite densities, makes it challenging to differentiate morphologically on peripheral blood smears.[12] The advent of polymerase chain reaction (PCR)-based diagnostics has improved detection of ovale infections, but initial PCR surveys across Africa and Asia based on the small subunit rRNA gene revealed two apparent groups of *P. ovale* parasites, termed classic and variant.[13] The discovery of perfect sequence segregation of 6 genomic markers, and more recently 12 mitochondrial loci, between classic and variant *P. ovale* isolates collected across Africa and Asia has led to the conclusion that this dimorphism actually represents a true species divide in the *P. ovale* clade.[14,15] The nomenclature of these species is currently evolving but will be referred to as *P. ovale curtisi* (*Poc*, formerly classic) and *P. ovale wallikeri* (*Pow*, formerly variant) herein.[16–18]

P. ovale curtisi and P. ovale wallikeri have since been confirmed to circulate within the same human populations throughout Africa and Asia,[19,20] with both detected by PCR at higher rates than previously appreciated.[5,12,21,22] Limited investigation of the genetic diversity and population genetics of the two *P. ovale* species have hinted at low diversity and/or small effective population size, as few unique haplotypes have been identified at antigenic gene targets like apical membrane antigen 1 (*ama1*) and merozoite surface protein 1 (*msp1*).[20,23] There is some indication that drugs used to treat *P. falciparum* are also shaping *P. ovale* parasite populations; signs of a selective sweep involving a mutant *dhfr* allele (implicated in pyrimethamine resistance) have been detected in both *Poc* and *Pow.*[24,25] Until now, the low density of most *P. ovale* isolates combined with lack of an *in vitro* culture system has hindered whole-genome sequencing of these parasites.[11] However, with development of strategies for parasite DNA enrichment, as well as construction of the first reference genomes in 2017, genome-wide analyses are now possible.[15,26–28]

We employed hybrid capture or leukodepletion to enrich *P. ovale* spp. DNA and perform whole-genome sequencing (WGS) of 25 clinical isolates collected from studies conducted across Ethiopia, the Democratic Republic of the Congo, Tanzania, and Cameroon. Combined with 20 additional public whole genomes from 11 countries spanning East, Central, and West Africa, we sought to better understand the comparative biology of *P. ovale curtisi*, *P. ovale wallikeri,* and co-endemic *P. falciparum* by examining their complexity of infection, population structure, nucleotide diversity, and genomic signatures of selection.

Results

High-quality genomic coverage of African *P. ovale* isolates

Parasite samples from 25 *P. ovale*-infected individuals collected at ten sites spanning Ethiopia, the Democratic Republic of the Congo (DRC), Tanzania, and Cameroon were selected for whole-genome sequencing (**Table 1**).[29–34] These included 13 *P. ovale curtisi* and 12 *P. ovale wallikeri* isolates that were selected from six studies based on robust amplification of the *po18S* rRNA gene (Ct <36) and predominance of one *ovale* species within each isolate. The majority of the samples (n=21) underwent a custom-designed hybrid capture with RNA baits to preferentially isolate ovale DNA extracted from dried blood spots for sequencing, while four additional whole blood samples were leukodepleted (LDB) at the time of collection by CF11 filtration and directly sequenced without enrichment.[35] Finally, genomic data of 20 *P. ovale* isolates sequenced as part of four previously-published studies were retrieved from the European Nucleotide Archive and the Sequence Read Archive.[15,28,36,37] These isolates either underwent selective whole-genome amplification (sWGA) or leukodepletion for parasite DNA enrichment prior to sequencing. Further data on all parasite isolates are found in **Supplemental Table 1**.

Study	Country of Origin	Year of Collection	Study Population	# selected for sequencing (# of *Poc* and *Pow*)
*hrp*2/3 Deletion Survey[29]	Ethiopia	2017- 2018	Febrile patients presenting to health facilities in the Amhara, Tigray, and Gambella regions	7 (2 *Poc*, 5 *Pow*)
SANRU Rural Health Program[30]	Democratic Republic of the Congo	2017	Febrile patients presenting to health facilities in Sud-Kivu, Bas-Uele, and Kinshasa Provinces	6 (2 *Poc*, 4 *Pow*)
Kinshasa Malaria Longitudinal Study[31]	Democratic Republic of the Congo	2015- 2017	Members of households participating in longitudinal study of malaria	5 (5 *Poc*)
TranSMIT[32]	Tanzania (East)	2018- 2022	Asymptomatic children and adults attending school or health clinics in rural Bagamoyo district, eastern Tanzania	4 (3 *Poc,* 1 *Pow*)
MSMT21[33]	Tanzania (West)	2020- 2022	Tanzanian citizens at health facilities	2 (2 *Pow*)
Dschang Febrile Cohort[34]	Cameroon	2020- 2021	Febrile patients presenting to health facilities in western Cameroon	1 (1 *Poc*)
Joste et al., *JID* 2023[36]*	Cameroon, Senegal, Ivory Coast	2013-2021	*P. ovale* infections identified in France after travel to an endemic country	4 (4 *Pow*)
Rutledge et al., *Nature* 2017[28]*	Ghana, Cameroon	Unknown	Symptomatic *P. falciparum* infected individuals with strong *P. ovale* signals among whole-genome sequencing results	2 (1 *Poc*, 1 *Pow*)
Higgins et al., *Sci Rep.* 2024[15]*	Tanzania, Kenya, South Sudan, Congo, Cameroon, Nigeria, Sierra Leone	2019- 2020	*P. ovale* infections identified in the United Kingdom after travel to an endemic country.	11 (6 *Poc*, 5 *Pow*)
Ansari et al., *Int J Parasitol.* 2016[37]*	Gabon, Nigeria	Unknown	Febrile Chinese males presenting to clinics in Jiangsu Province, China, after travel to an endemic country	3 (1 *Poc*, 2 *Pow*)

Table 1. Studies of origin for 45 *P. ovale* isolates.
*Raw sequencing data for these 20 isolates were directly incorporated into the analysis pipeline after retrieval from the European Nucleotide Archive or NCBI Sequence Read Archive.

Whole-genome sequencing achieved high genome coverage, with an overall average of 86% and 87% ten-fold coverage across the core genome for the 21 *P. ovale curtisi* and 24 *P. ovale wallikeri* isolates, respectively (**Figure 1**). Coverage and mapping proportion were highest when aligned to the *P. ovale* reference genome determined by the *Poc*/*Pow* species-specific qPCR assay, corroborating initial species assignment. Compared to sWGA and LDB samples, the hybrid capture method used to enrich parasite DNA in the majority of samples yielded more complete coverage across all chromosomes except for chromosome 10 (**Figure 1**). The hybrid capture was originally designed for *P. ovale wallikeri*, with additional *P. ovale curtisi* baits then selected to cover areas that differ between the two ovale genome assemblies (PowCR01 and PocGH01).[28] Due to *Pow* chromosome 10 being incomplete in the PowCR01 reference genome (only 470kb), this approach did not provide coverage for the full *Poc* chromosome 10 (1,300kb).

This led to substantially lower coverage for chromosome 10 across all *Poc* hybrid capture isolates (40-60% 10x coverage vs. >85% for all other *Poc* chromosomes); thus, chromosome 10 was excluded from all genome-wide analysis in *Poc* isolates to limit error.

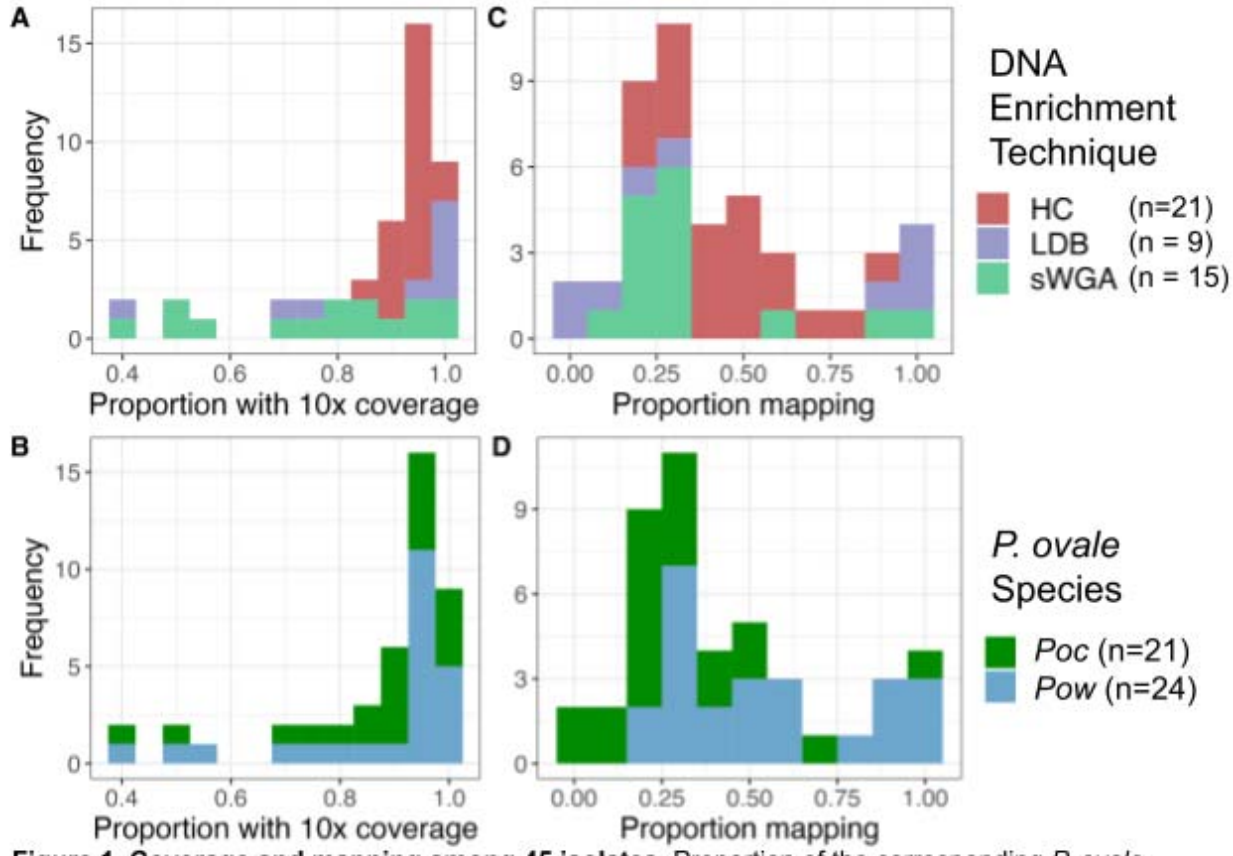

Figure 1. Coverage and mapping among 45 isolates. Proportion of the corresponding *P. ovale* reference genome covered by ≥10 reads by DNA enrichment technique (A) and species (B). Proportion of reads mapped to that reference genome by DNA enrichment technique (C) and species (D). For *Poc*, chromosome 10 was excluded due to incomplete coverage by hybrid capture baits. Five samples from *Higgins et al.* were not incorporated into this study due to having <30% 10x coverage of the corresponding genome. HC = hybrid capture; LDB = leukodepleted blood; sWGA = selective whole-genome amplification

As, expected, hybrid capture led to preferential sequencing of *P. ovale* DNA among samples that were co-infected with *P. falciparum* (*Pf*); *Pf*-positive isolates that underwent hybrid capture yielded only 2-11% 10x coverage of the *Pf* genome compared to >90% 10x coverage of the *Pf* genome among leukodepleted blood samples. For genomic analysis, insertions/deletions, multiallelic sites, low-quality variants, and variants within tandem repeats and expanded gene families were excluded (see **Methods**), yielding final biallelic single nucleotide polymorphism (SNP) call sets of 73,015 SNPs for *P. ovale curtisi* and 45,669 for *P. ovale wallikeri*.

Low complexity of infection

Complexity of infection (COI), or the number of unique parasite clones present in a given isolate, was estimated 1000 times using THEREALMcCOIL for all 21 *P. ovale curtisi* and 24 *ovale wallikeri* isolates, as well as 2,077 geographically matched *P. falciparum* isolates

downloaded from the publicly available MalariaGEN Pf6 dataset (**Figure 2**).[38] Twenty out of 21 *Poc* isolates (95%) and 23 out of 24 *Pow* isolates (96%) were estimated to be monoclonal; the remaining isolate in each *P. ovale* species was found to comprise two parasite clones. By comparison, roughly half (1,165/2,077; 56%) of *P. falciparum* samples were monoclonal. COI differed significantly (p = 0.005) among the three *Plasmodium* species. In pairwise comparisons, both *Poc and Pow* had significantly lower COI compared to *P. falciparum* (p = 0.001 and p=0.004, respectively).

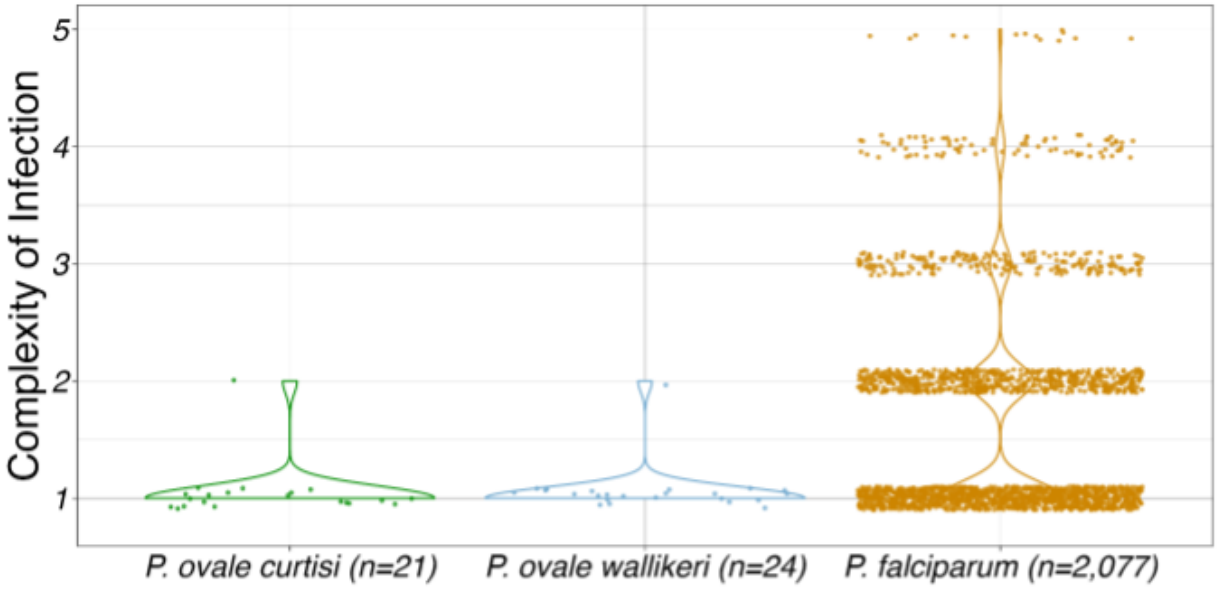

Figure 2. Median estimated complexity of infection (COI) among 21 *Poc* isolates, 24 *Pow* isolates, and 2,077 *P. falciparum* isolates geographically matched to the *P. ovale* samples by country of origin. The distributions of COI differed significantly among the three species (p < 0.0001) with *Pow* and *Poc* showing significantly lower COI than *P. falciparum* (p = 0.0004 and 0.012, respectively). Average read depth of coverage for *Poc*, *Pow*, and *Pf* isolates were 44.1, 95.7, and 147.5, respectively.

The two multiclonal *P. ovale* infections were both hybrid-capture-enriched, high coverage (94% and 98% 10-fold coverage in *Poc* and *Pow*, respectively) and came from high-transmission areas of the DRC;[39] each had a COI of 2. In order to determine whether the two clones in these samples were distinct lineages or meiotic siblings, we analyzed the distribution of heterozygous SNPs across the genome. We hypothesized that meiotic siblings would only have heterozygous SNPs in specific regions, reflecting recombination within the mosquito midgut.[40] In both samples, after filtering to high confidence SNPs based on population-wide allele frequency, we saw an even distribution of heterozygous SNPs across the genome, suggestive of two distinct parasite lineages in the same host rather than meiotic siblings (**Supplemental Figure 1**).

Lower nucleotide diversity in *P. ovale wallikeri* compared to *P. ovale curtisi*

Among a collection of 3,339 sets of one-to-one-to-one orthologous genes between the *Poc*, *Pow*, and *P. falciparum* genomes, we identified 2,008 sets that achieved high-quality sequencing coverage and had no overlap with masked genomic regions in any of the three

species. The average species-specific nucleotide diversity (□) among these orthologues in the 20 monoclonal *Poc*, 23 monoclonal *Pow*, and 19 geographically-matched monoclonal *Pf* samples were 2.9×10^{-4}, 1.8×10^{-4}, and 2.6×10^{-4}, respectively. These were significantly different between species ($p < 0.0001$, $F = 98$, $df = 2$), with orthologues in *P. ovale curtisi* more diverse than in *P. ovale wallikeri* and *P. falciparum* (p-values <0.0001 and 0.002, respectively), and *Pow* orthologues less diverse than in *Pf* ($p < 0.0001$) (**Figure 3A**). To mitigate bias by geographic coverage and orthology with the *P. falciparum* genome, we repeated this analysis using 2,911 *Poc-Pow* orthologues among a group of geographically-matched monoclonal *Poc* and *Pow* samples (n=11 each, **Supplemental Table 3**), revealing average nucleotide diversities of 2.5×10^{-4} and 1.8×10^{-4}, respectively (**Figure 3B**). Nucleotide diversity was still significantly lower in *Pow* orthologues compared to *Poc* ($p < 0.0001$).

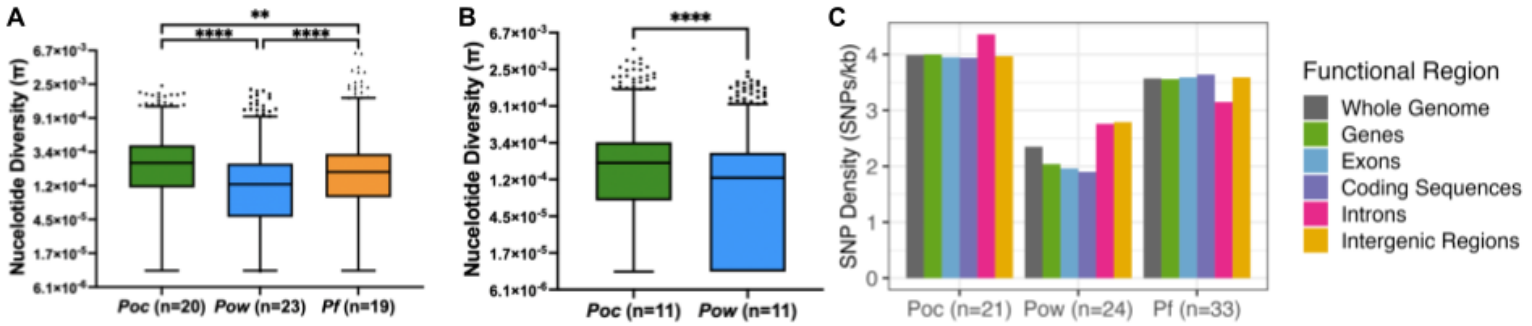

Figure 3. Nucleotide diversity (π) of orthologous genes and SNP density by functional genomic region among *Poc*, *Pow*, and *P. falciparum* (*Pf*) isolates. (A) Nucleotide diversity (π) per gene among 2,008 sets of orthologous genes in monoclonal *Poc*, *Pow*, and *Pf* samples. Boxes denote 25th, median, and 75th percentiles; whiskers drawn at 1st and 99th percentiles. π of 0 was coded as $1x10^{-5}$ to plot on logarithmic scale. Nucleotide diversity was significantly different between orthologues of all three species by Tukey's multiple comparisons tests, with *Poc* orthologues showing higher diversity than orthologues of *Pow* and *P. falciparum*, and *Pow* orthologues also showing lower diversity than those in *P. falciparum* (p-values < 0.002). (B) Nucleotide diversity (π) per gene among 2,911 sets of orthologous genes in geographically-matched monoclonal *Poc* and *Pow* samples. Nucleotide diversity was significantly lower among *Pow* orthologues compared to *Poc* (p < 0.0001). (C) SNP density in different functional regions of the genome among all *Pow*, *Poc*, and *P. falciparum* isolates. SNP = single nucleotide polymorphism; kb = kilobase.

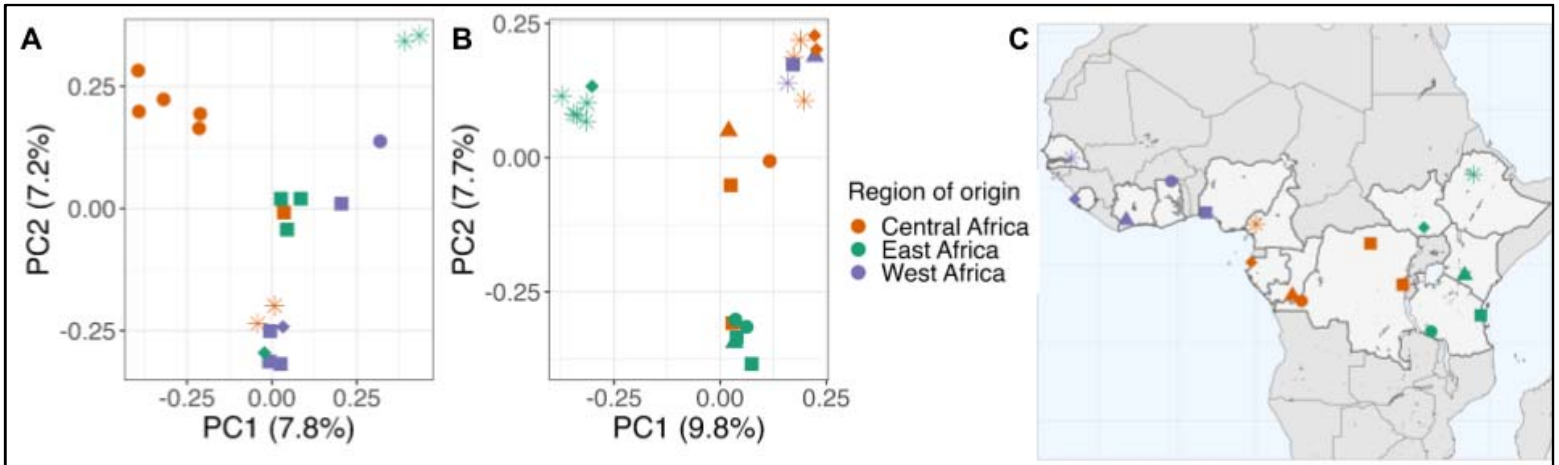

Figure 4. Principal component analysis showing the first two principal components among 20 monoclonal *Poc* isolates (A) and 23 monoclonal *Pow* isolates (B) using 4,116 and 3,189 biallelic SNPs, respectively. Samples colored by region of country of origin; in the map, parasites from travelers are assigned to capital city (C). In PC2 of *Pow*, SNPs within both the *ts-dhfr* and *mrp1* gene were among the top 0.5% of contributors.

This high nucleotide diversity in *P. ovale curtisi* was consistent with investigation of the total number and density of genome-wide SNPs. Variant calling and filtering resulted in almost twice the number of SNPs for *P. ovale curtisi* (73,015) as for *P. ovale wallikeri* (45,669), despite a slightly smaller number of *Poc* isolates (21 vs. 24). This corresponded to a higher density of SNPs across the *Poc* genome (4.0 SNPs per kilobase[kb] in *Poc* vs. 2.4 SNPs/kb in *Pow*). However, a smaller proportion of SNPs in the *Poc* genome were nonsynonymous mutations, as the ratio of nonsynonymous-to-synonymous (dN/dS) mutations was 1.5 and 2.5 in *Poc* and *Pow*, respectively. Among the aforementioned geographically-matched *P. ovale* isolates, dN/dS within 2,911 orthologous genes was 1.4 for *Poc* and 2.5 for *Pow*, consistent with the broader estimates. SNP densities in both the *Poc* and *Pow* genomes were lowest in protein-coding sequences (3.9 and 1.9 SNPs/kb, respectively), and higher in introns (4.4 and 2.8 SNPs/kb) (**Figure 3C**). Intergenic regions in *Poc* showed relatively lower SNP density similar to protein-coding sequences (4.0 SNPs/kb), but these same regions in *Pow* had relatively high SNP density similar to introns (2.8 SNPs/kb).

Parasite genomic similarity recapitulates geographic relationships

Genome-wide principal component (PC) analysis of the monoclonal samples of each ovale species revealed spatial arrangement of related parasites along PC1 and PC2 that aligns with their location of origin (**Figure 4**). These components accounted for 15.0% and 17.5% of the genetic differentiation in *Poc* and *Pow*, respectively. While cluster analysis by ADMIXTURE found the best fit when modeling each isolate as a separate cluster, except for one pair of isolates per species originating from the capital of Kinshasa in the DRC (in *Poc*) and the Amhara region in Ethiopia (in *Pow*), geographic alignment was evident in the PCA. For *Pow*, PC1 and PC2 appear to reflect an East-West axis and North-South axis, respectively, with samples from Ethiopia and South Sudan in the west divided from others by PC1. In the PCA for *Poc*, Ethiopian parasites also organized separately from other samples, as did isolates from Kinshasa in the DRC. The remaining *Poc* samples show some division between East, Central, and West Africa, though the alignment with geography is less consistent than in *Pow.* In both *P. ovale* spp., PC3 and PC4 further separated samples from various countries (**Supplemental Figure 2**).

Examination of the top 0.5% of variants by contribution to each of the first 4 principal components revealed that SNPs within genes encoding multidrug resistance protein 1 (*mdr1*) and dihydrofolate reductase - thymidylate synthase (*dhfr-ts*), two putative antimalarial resistance genes, were major contributors to the North-South axis in *Pow* PC2. Among all 24 *Pow* samples, three previously-documented haplotypes in *Pow dhfr-ts*, a key gene in folate metabolism that is implicated in pyrimethamine resistance,[41,42] appear to drive this geographic differentiation, with the Phe57Leu+Ser58Arg haplotype existing in in 45% of our Central African clones and 36% of our East African clones but none of the sequenced West African clones (**Supplemental Figure 3A**).[25] This haplotype is associated with resistance to pyrimethamine when expressed in *E. coli*. Though it did not drive differentiation in the PCA, *Poc dhfr-ts* haplotypes similarly showed presence of a putative drug resistance haplotype (Ala15Ser+Ser58Arg) in the Central and East African clones but not in West Africa, though our

sample size for West Africa was general smaller for both species (three and six isolates in *Pow* and *Poc*, respectively) (**Supplemental Figure 3B**).

Signatures of selection contain putative drug resistance loci, proteins involved in sexual stage differentiation, and antigenic targets

We calculated nS_L and Tajima's D across the genomes to identify loci under directional and balancing selection, respectively. The nS_L statistic is considered robust to the currently-unknown recombination rates across the genomes of *P. ovale* species.[43] Genetic markers of interest within 10kb of the top 0.5% absolute normalized nS_L values that may be influenced by selective sweeps are listed in **Table 2** and **Table 3**. Evidence of a selective sweep involving the putative bifunctional dihydrofolate reductase - thymidylate synthase (*dhfr-ts*) gene[41,42] was found in both *P. ovale* species (**Figure 5**). Examination of extended haplotype homozygosity (EHH) at the selected variants show a large selective sweep in *Pow* spanning roughly 40kb as well as close proximity of the *dhfr-ts* gene to the focal variant (**Figure 6A, 6B**). In *Poc*, the positioning of the *dhfr-ts* gene lies at the edge of a smaller sweep (**Figure 6C, 6D**). However, another putative marker of drug resistance, multi-drug resistance associated protein 2 (*mrp2*), was found in close proximity to one of the highest absolute normalized nS_L value in *Poc* and lies near the center of a 40kb sweep region on *Poc* chromosome 14 (**Figure 6E, 6F**).

Statistic	Value	Chr.	Location	Closest plausible genetic driver	Distance	Gene ID
nS_L	5.99	1	127675	HECT-type E3 ubiquitin ligase UT, putative (*ut*)	1798	PocGH01_01012400
	-3.47	1	203583	cysteine-rich secretory protein, putative (*crisp*)	-4763	PocGH01_01013600
	-3.61	3	541949	cysteine repeat modular protein 2, putative (*crmp2*)	6695	PocGH01_03022100
	-3.40	5	66310	early transcribed membrane protein, putative (*etramp*)	-790	PocGH01_05011300
	-3.38	5	107531	GPI-anchored micronemal antigen, putative (*gama*)	-3142	PocGH01_05012100
	-3.71	5	774030	bifunctional dihydrofolate reductase-thymidylate synthase, putative (*dhfr-ts*)	-9660	PocGH01_05028400
	-3.65	9	1197220	apical membrane antigen 1, putative (*ama1*)	605	PocGH01_09039800
	-3.55	12	703579	merozoite surface protein 7-like protein, putative (*msp7*)	1983	PocGH01_12027700
	-4.03	12	2760110	male development protein, putative (*md1*)	0	PocGH01_12076000
	-4.01	14	1607839	AP2 domain transcription factor, putative (*ap2-g*)	-4111	PocGH01_14048300
	-5.25	14	1899110	ABC transporter C family member 2, putative (*mrp2*)	7715	PocGH01_14054800
Tajima's D	2.66	7	1152840	merozoite surface protein 1, putative (*msp1*)	0	PocGH01_07037900

Table 2. Selection statistics and nearby genetic markers for loci with top normalized nS_L and positive Tajima's D values among monoclonal isolates of *Poc*. Loci are described by chromosome (chr.), location on the chromosome in base pairs, and a statistical value in the top 0.5% across the genome. Nearby genetic markers were identified within 10,000 base pairs of these loci and are given alongside their gene ID and the distance of this marker to the reported locus (negative distance indicates upstream location).

1

Statistic	Value	Chr.	Location	Closest plausible genetic driver	Distance	Gene ID
nS_L	-4.61	2	537994	dynein heavy chain, putative (*dhc*)	0	POWCR01_020017200
	-4.79	2	554712	transcription factor with AP2 domain(s) (*apiap2*)	7318	POWCR01_020017600
	-5.08	3	554677	dynein heavy chain, putative (*dhc*)	2069	POWCR01_030017700
	-4.99	4	603847	merozoite surface protein 5, putative (*msp5*)	-5083	POWCR01_040018700
	-4.89	5	846693	bifunctional dihydrofolate reductase-thymidylate synthase, putative (*dhfr-ts*)	-953	POWCR01_050023500
	-4.69	7	456511	cysteine repeat modular protein 1, putative (*crmp1*)	-6204	POWCR01_070013600
	-5.45	7	1080681	dynein light chain, putative (*dhc*)	8560	POWCR01_070029300
	-5.22	8	1135323	6-cysteine protein B9 (*6-cys*)	4768	POWCR01_080029500
	-4.39	9	792065	dynein heavy chain, putative (*dhc*)	0	POWCR01_090024400
	-4.93	12	525249	sporozoite protein essential for cell traversal, putative (*spect1*)	-5947	POWCR01_120016200
	-4.10	13	177064	*Plasmodium* interspersed repeat protein (*pir*)	-5114	POWCR01_130008000
	-4.10	13	177064	early transcribed membrane protein, putative (*etramp*)	6011	POWCR01_130008100
Tajima's D	2.55	1	31910	conserved Plasmodium protein, unknown function	0	POWCR01_010005700
	2.58	1	128700	serine/threonine protein kinase, putative	0	POWCR01_070032200
	2.13	7	1184250	merozoite surface protein 1, putative (*msp1*)	0	POWCR01_080035700
	2.81	12	235390	stromal-processing peptidase, putative	0	POWCR01_130008300

Table 3. Selection statistics and nearby genetic markers for loci with top normalized nS_L and positive Tajima's D values among monoclonal isolates of *Pow.* Loci are described by chromosome (chr.), location on the chromosome in base pairs, and a statistical value in the top 0.5% of absolute values across the genome. Nearby genetic markers were identified within 10,000 base pairs of these loci and are given alongside their gene ID and the distance of this marker to the reported locus (negative distance indicates upstream location).

1

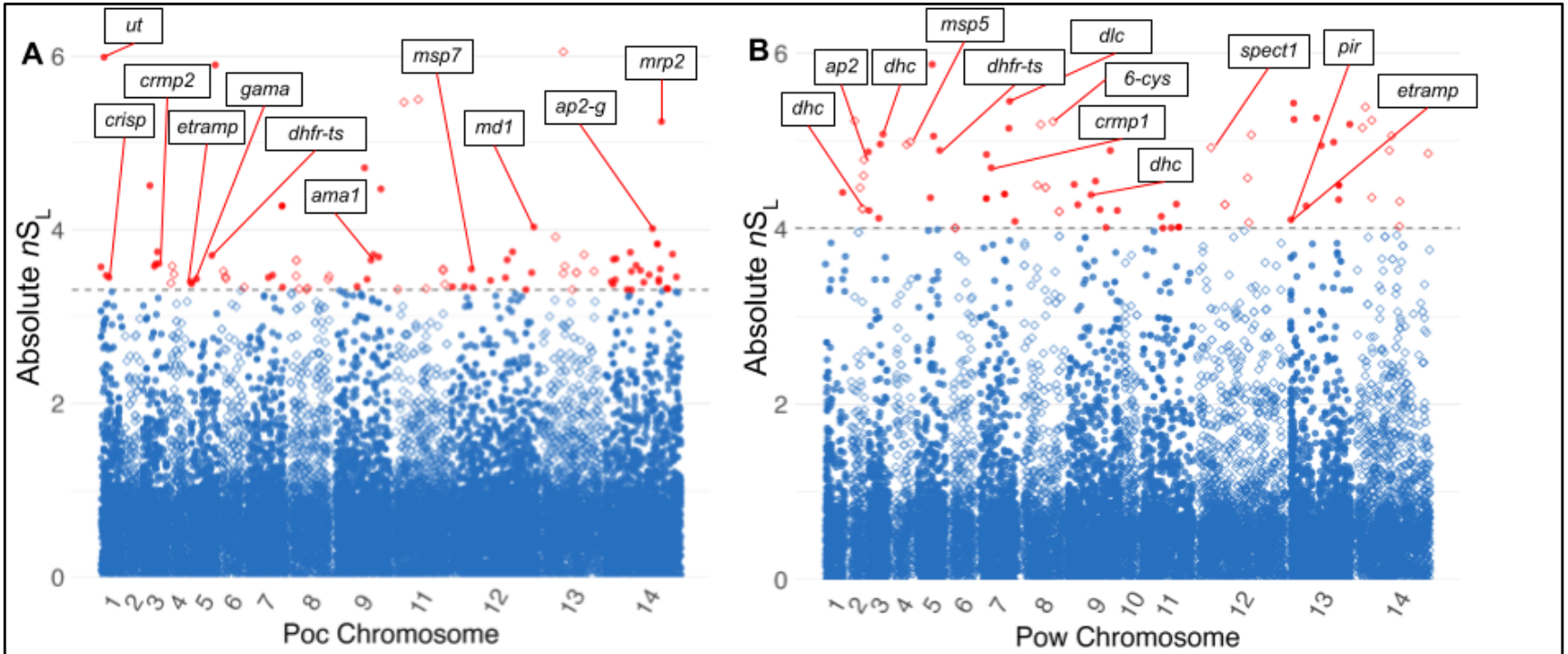

Figure 5. Absolute nS_L of 19,205 variants among monoclonal isolates across the *Poc* genome (A) and 15,744 variants among monoclonal isolates across the *Pow* genome (B). Individual loci are depicted using alternating shapes between chromosomes for legibility. Dotted line and red color denote the top 0.5% of loci. Putative genetic markers of note within 10,000 bases of these loci are labelled, including ubiquitin transferase (*ut*), cysteine-rich secretory protein (*crisp*), cysteine repeat modular protein 2 (*crmp2*), early transcribed membrane protein (*etramp*), GPI-anchored micronemal antigen (*gama*), dihydrofolate reductase - thymidylate synthase (*dhfr-ts*), apical membrane antigen (*ama1*), merozoite surface protein 7-like protein (*msp7*), male development protein 1 (*md1*), AP2 domain transcription factor G (*ap2-g*), multi-drug resistance associated protein 2 (*mrp2*), dynein heavy chain (*dhc*), AP2 domain transcription factors (*ap2*), merozoite surface protein 5 (*msp5*), cysteine repeat modular protein 1 (*crmp1*), dynein light chain (*dlc*), 6-cysteine protein (*6-cys*), sporozoite protein essential for cell traversal 1 (*spect1*), *Plasmodium* interspersed repeat protein (*pir*), and early transcribed membrane protein (*etramp*).

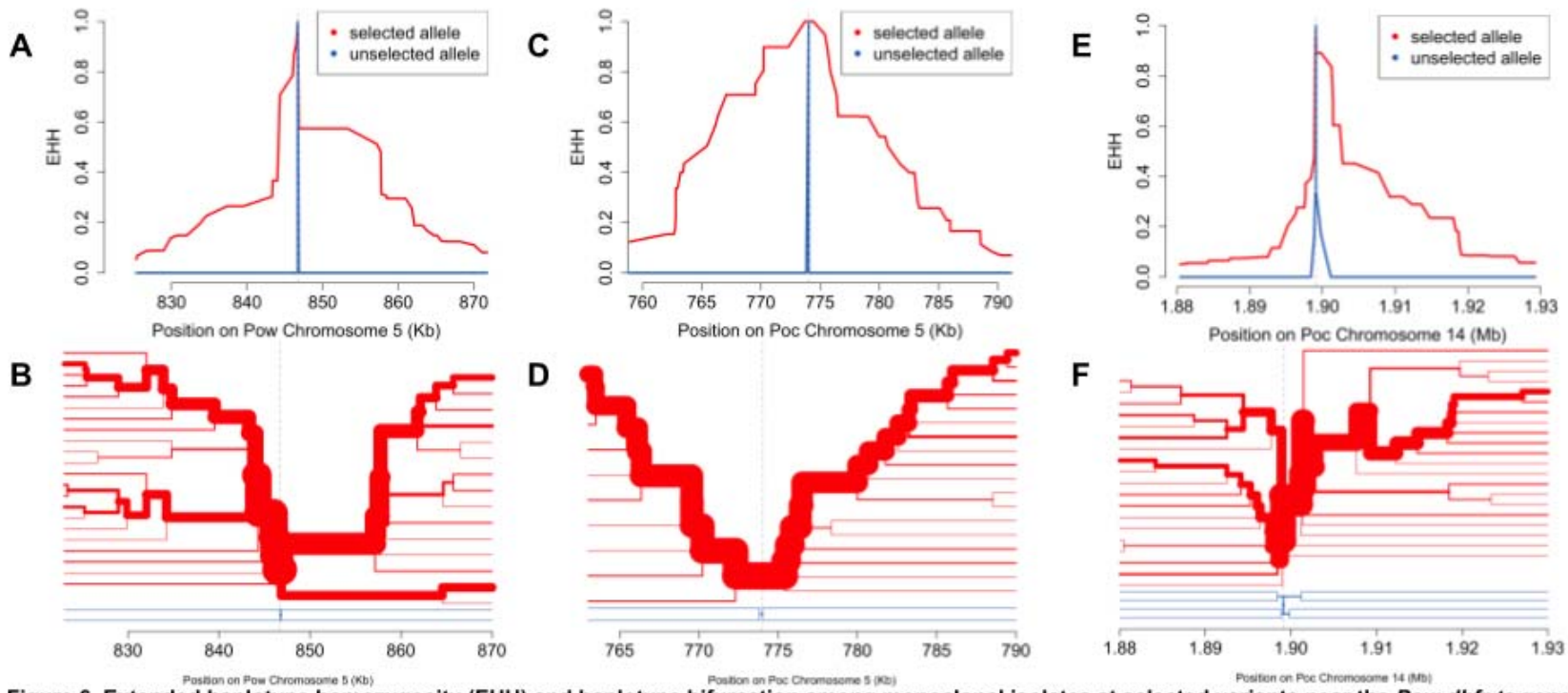

Figure 6. Extended haplotype homozygosity (EHH) and haplotype bifurcation among monoclonal isolates at selected variants near the *Pow dhfr-ts* gene (A, B), the *Poc dhfr-ts* gene (C, D), and the *Poc mrp2* gene (E,F). EHH and haplotype bifurcation show selective sweeps spanning ~30kb, ~40kb, and ~30kb, respectively, with lineage breakdown occurring first among the unselected allele haplotypes (blue) and then in the selected allele haplotypes (red) as distance from the focal variant increases.

Top absolute nS_L hits were also found near *ap2* transcription factor genes that regulate apicomplexan life cycle transitions, including sexual differentiation into gametocytes (*ap2-g*), and genes involved in sex-specific development of gametes, such as those coding male development protein 1 (*md1*) and cysteine-rich secretory protein (*crisp*).[44–46] In *Pow*, four top nS_L hits were found around genes encoding the dynein heavy and light chains, cytoskeleton components highly expressed in male gametes for motility and fusion with female gametes in the mosquito blood meal.[47] Top nS_L hits were also found near cysteine-repeat modular proteins 2 and 1 (*crmp2*/*1)* in *Poc* and *Pow*, respectively, proteins which may be involved in targeting sporozoites to the salivary glands in the mosquito prior to transmission.[48,49]

Finally, genes encoding putative antigenic targets at the host-parasite interface, including merozoite surface protein 7 (*msp7*), merozoite surface protein 5 (*msp5*), early transcribed membrane protein (*etramp*), apical membrane antigen 1 (*ama1*), GPI-anchored micronemal antigen (*gama*), and 6-cysteine protein B9 (*6-cys*) may be under directional selection in both *P. ovale* species.[50,51] An orthologue of sporozoite protein essential for cell traversal 1 (*spect-1*), a protein necessary for liver cell invasion that has been investigated as a potential vaccine target,[52] was also among the top hits in *Pow*.

Overall, Tajima's D in both species exhibited a negative skew across the genome with an average value of -1.06 for *Poc* and -0.78 for *Pow*. This may suggest population expansion following a bottleneck or weak directional selection (**Figure 7**). Among the loci with positive values in the top 0.5% of absolute Tajima's D hits, the antigenic marker merozoite surface protein 1 (MSP1) was identified as a probable target of balancing or diversifying selection in both *P. ovale* species (**Tables 2, 3**).

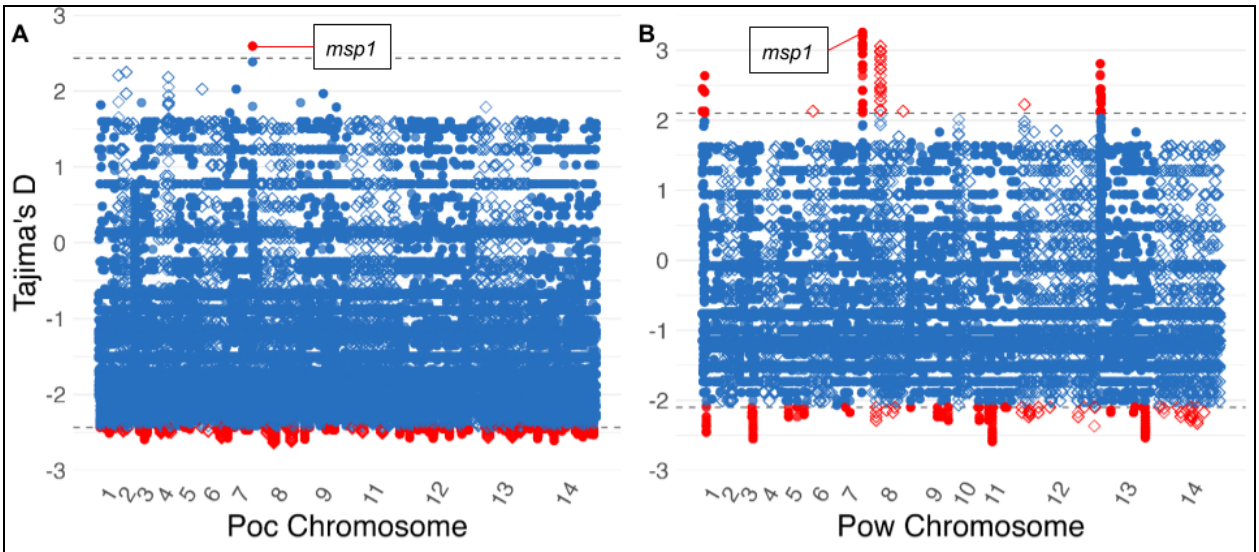

Figure 7. Tajima's D in 399,355 and 297,286 300bp windows in genes across the *Poc* (A) and *Pow* (B) genomes among monoclonal isolates. Individual windows are depicted using alternating shapes between chromosomes for legibility. Dotted line and red color denote the top 0.5% of loci. For both species, the top locus with a positive Tajima's D was located inside the merozoite surface protein 1 (*msp1*) gene.

Discussion

We present a comprehensive population genomic study of both *P. ovale* species within sub-Saharan Africa. Our study comprises 21 *Poc* and 24 *Pow* isolates selected from 11 studies, including both febrile and asymptomatic cases. Genome-wide analysis reveals differences in nucleotide diversity between *P. ovale* species, but similarity in their low complexity of infection, geographic relatedness, and signatures of selection. Our analysis was performed using genomic enrichment methods specifically designed to enable robust coverage and analysis with the 2017 reference genomes of *P. ovale curtisi* (from Ghana) and *P. ovale wallikeri* (from Cameroon), which were the available references at the time of the study.[28]

Compared to the "classic" *P. ovale curtisi* species, we observed significantly lower nucleotide diversity across orthologous genes among geographically-matched *P. ovale wallikeri* isolates (2.5×10^{-4} for *Poc* and 1.8×10^{-4} for *Pow*, respectively). Our estimate for *Poc* is concordant with the genome-wide diversity calculated among six Central African *Poc* isolates[15] as well as that derived from RNA expression data among four parasite samples from Mali.[53] However, our *Pow* estimate was substantially lower than the genome-wide estimate reported by Higgins et al. (3.4×10^{-4}), despite our inclusion of their samples alongside additional Central and East African isolates. Our lower estimate may reflect the exclusion of higher-diversity intergenic regions, though we also found lower genome-wide and intergenic SNP density in *Pow* compared to *Poc.* Relatively low nucleotide diversity in *Pow* may indicate reduced effective population size, increased inbreeding, or a population bottleneck in the time since *Poc* and *Pow* diverged between 1.3 and 20.3 million years ago.[14,28] More recent population growth in both species is also suggested by the predominantly negative distribution of Tajima's D values across their protein-coding genes, a finding that can indicate population expansion following a bottleneck.[54] The high ratio of nonsynonymous-to-synonymous substitutions among these protein coding genes (2.5 for *Pow*, 1.5 for *Poc*) is similar to that seen in *P. falciparum* and *P. vivax.*[55,56] This finding may represent diversifying selection on proteins across either *P. ovale* genome, enabling maintenance of nonsynonymous substitutions, or inflation of dN/dS ratios observed among *Plasmodium* parasites due to the impact of the malaria life cycle on allele frequencies.[57] Further analysis of subpopulations of each parasite species could help to elucidate the factors driving the observed difference in genomic diversity, such as by determining whether *Pow* isolates from Asia have similarly low nucleotide diversity or if this finding is specific to Africa.

The observed predominance of monoclonal isolates among both *P. ovale* species is consistent with low within-sample haplotypic diversity seen in previous investigations of African *P. ovale* isolates by genome-wide RNA sequencing and amplicon sequencing.[53,58] Low complexity of *P. ovale* infections may result from efficient clonal transmission[32] and/or lower transmission overall, limiting vector uptake of multiple parasite clones from either the same or different infected individuals. This low complexity is expected to limit opportunities for genetic recombination within mosquito vectors, though multiple-clone infections were identified in Kinshasa, a region with overall higher malaria endemicity and transmission intensity.[39]

Genomic signatures of selection within both *P. ovale* species highlighted the importance of antimalarials, host-vector life cycle transitions, and human immunity as evolutionary pressures impacting parasite survival. *P. ovale* infections are frequently subclinical and go untreated,[59] but likely still face substantial drug exposure from widely used antimalarials prescribed for *P. falciparum.*[22] Additionally, malaria prophylaxis using sulfadoxine-pyrimethamine, such as intermittent preventive therapy in pregnancy (IPTp) and seasonal malaria chemoprevention for infants and schoolchildren (SMC), may be applying drug pressure on *P. ovale* parasite populations.[1] Selective sweeps in *dhfr-ts*, a gene implicated in resistance to pyrimethamine, have been documented in both *Poc* and *Pow*, and certain mutant alleles were found to confer pyrimethamine resistance when expressed in *E. coli*.[24,25] In our dataset, sweeps near the *dhfr-ts* genes were among the strongest signals of directional selection in both *P. ovale* species, especially in *Pow*, possibly representing drug pressure influencing parasite survival. We also found the putative pyrimethamine resistance *Pow dhfr-ts* haplotype Phe57Leu+Ser58Arg to be a major contributor to principal component 2 of *Pow* (representing the North-South axis); the resistant haplotype composed 36% (9/25) of our *Pow* haplotypes, with representation in Central and East Africa but no detection in West Africa. Another putative pyrimethamine resistance haplotype (Ala15Ser+Ser58Arg) in *Poc* was similarly detected in East and Central Africa, though not in West Africa.[25] Functional evaluation of different alleles to determine their capacity to confer drug resistance, as well as monitoring of these alleles across the parasite populations over time, will further clarify how interventions targeting *P. falciparum* may be simultaneously rendering *P. ovale* parasites harder to control.

Finally, strong signals of balancing or diversifying selection were observed in both species within their genes encoding merozoite surface protein 1 (MSP1), the orthologues of the predominant antigen on blood-stage *P. falciparum* parasites that has been shown to induce protective immunity in some studies.[60] Diversifying selection on MSP1 has been documented in *P. falciparum*[61] as well as in focused analysis among African *P. ovale* infections imported to China.[62] Our dataset provides even stronger evidence for diversifying selection at this site, as the *msp1* gene showed the single highest Tajima's D value across all genes in both *P. ovale* species. Such immune responses may also play a role in modulating relapse potential.[63]

This study has several limitations. While it represents the largest genome-wide examination of the genomic composition of both *P. ovale curtisi* and *P. ovale wallikeri* to date, the sample size for both species is nonetheless small and limits the power to detect clustering of isolates, infer population demography, and detect selection. The geographic coverage of the isolates employed differs between the 13 countries represented, and isolates from Northern or Southern Africa were not available. Whole-genome enrichment methods also differed among isolates; 21 isolates employed hybrid capture, 15 used selective whole-genome amplification, and nine relied on leukodepletion. The two former methods may have induced amplification bias, whereas leukodepletion does not amplify *P. ovale* DNA and therefore may reduce the power to identify rare variants in those isolates. Disparate average read depth between the three species (44.1, 95.7, and 147.5 for *Poc*, *Pow*, and *Pf*, respectively) may also have differentially impacted our ability to detect polyclonal infections, but the low complexity of infection found in both *P. ovale* species should be robust given the satisfactory sequencing

depth overall. The source studies also differ by whether samples were derived from asymptomatic carriers (n=11) or febrile patients (n=34). Sample sizes were too small to analyze these populations separately. Finally, hybrid capture baits designed using the incomplete PowCR01 reference genome led to incomplete coverage of *Poc* chromosome 10, which was excluded from analyses. Unfortunately, newly-assembled regions of *Pow* chromosome 10 were not available during the analysis. The hybrid capture approach also did not enable enrichment and analysis of loci in the mitochondrial and apicoplast genomes, which were excluded from analysis. We do not expect these exclusions to systematically bias estimation of nucleotide diversity nor complexity of infection, though it does prevent us from evaluating excluded loci (including *mdr1*, *msp3*, and *msp8*) for genomic signatures of selection. The availability of selective whole genome amplification protocols now provides a less expensive approach to targeted DNA enrichment for *P. ovale* spp. that does not rely on the specific design of hybrid capture baits.[27]

This study provides a comparative genomic analysis of the two *Plasmodium ovale* species sympatrically circulating in sub-Saharan Africa and presents new evidence of selective pressures on genes related to drug response, sexual differentiation, and immune evasion. Further population genomic studies of *Poc* and *Pow* should employ a larger selection of isolates from a greater geographic range, especially including Asia, and take advantage of new reference genome assemblies to build on these insights.[15] Functional investigation into the genes showing signatures of selection, including via orthologue replacement in closely related *Plasmodium* species,[64,65] is also an exciting new strategy in substantiating the biological relevance of key loci, with implications for transmission prevention, treatment strategies, and vaccine development for *P. ovale* spp. Finally, cataloging genome-wide diversity facilitates the design of targeted genotyping methods that can efficiently characterize the epidemiology of these understudied parasite species.[66] Combining these approaches to better evaluate *P. ovale* parasite relatedness, transmission, and relapse patterns can help to improve the impact of current malaria control strategies on all human-infecting malaria species.[36,67,68]

Methods

Sample selection

Clinical isolates in the form of dried blood spots or leukodepleted blood were drawn from six studies shown in **Table 1**, including studies involving both asymptomatic persons and febrile patients across four countries. Across these studies, participants were screened for the presence of *P. ovale* spp. infection by a real-time polymerase chain reaction (qPCR) assay targeting the *po18S* rRNA gene.[22] Among 282 isolates with a *po18S* Ct value under 40, a species-specific (*Poc* and *Pow*) 18S rRNA qPCR assay was employed to determine the ovale species present.[69] Candidates were selected from isolates with only one species detected or mixed infections in which one species predominated by ≥3 Ct (corresponding to approximately 8 times as much DNA). Samples were also screened for presence of *P. falciparum* co-infection using a qPCR assay for the *pfldh* or *pf18S* rRNA gene.[31,39] Ultimately, samples from 25 individuals were selected for whole-genome sequencing based on higher-density *P. ovale* infection, lack of or lower-density *P. falciparum* coinfection, and balance of ovale species and

geographic diversity across the sample set. Characteristics of these 25 samples, and an additional 20 samples from four previously-published studies,[15,28,36,37] are shown in **Supplemental Table 1**.

Library preparation and sequencing

DNA extracted from dried blood spots using a Chelex protocol[70] was sheared to 300bp using a LE220R-plus Covaris Sonicator (Covaris, Woburn, MA). Fragment size was checked with an Agilent TapeStation 4150 (Agilent, Santa Clara, CA) and DNA concentrations were tested using a Qubit Flex fluorometer (Thermo Fisher Scientific, Waltham, MA). Isolates were then prepared for sequencing using the KAPA Hyperprep kit (Kapa Biosystems, Woburn, MA). Four Tanzanian DNA isolates extracted from blood that had been leukocyte-depleted by CF11 filtration at the time of collection[35] were directly incorporated into sequencing libraries. The remaining 21 isolates derived from dried blood spots were additionally processed using a custom-designed hybrid capture protocol to enrich for ovale DNA via thousands of RNA probes specifically designed to amplify *P. ovale* DNA without binding to human DNA (Twist Bioscience, San Francisco, CA, USA). Hybrid captures probes were designed first for the *P. ovale wallikeri* genome (PowCR01), with unique probes added for the *P. ovale curtisi* genome (PocGH01) at any sites that differed by more than 10% of bases.[28] Since the reference genome for chromosome 10 is significantly smaller for *Poc* compared to *Pow* (roughly 1,300kb vs 470kb, respectively), this bait design approach led to a lack of baits covering 63% of *Poc* chromosome 10. Chromosome 10 was therefore excluded from analysis of *Poc* isolates. Captures were performed with four samples per capture. After preliminary sequencing on a Miseq Nano flow cell (Illumina, San Diego, CA, USA), libraries were sequenced on the Novaseq 6000 S Prime (Illumina, San Diego, CA, USA) sequencing system with 150bp paired-end chemistry. Samples from Joste et al. and Higgins et al. included in our analysis were enriched using selective whole genome amplification (sWGA), employing sets of 5-10 primers designed to preferentially amplify the PowCR01 and PocGH01 genomes over human background DNA.[71]

Sequencing data alignment and variant calling

Data processing and analysis were performed in the bash environment using a python-based *snakemake* v7.24.2 wrapper for pipeline construction, automation, and reproducibility.[72] Following trimming and quality control, a “dual” reference genome was produced for each *P. ovale* species by concatenating the reference genome of that ovale species (*P. ovale curtisi: PocGH01; P. ovale wallikeri: PowCR01*) to the *P. falciparum* strain *Pf3D7* reference genome.[28,73] Alignment and deduplication of sequencing data was performed following the *GATK* v4.4.0.0 best practices pipeline.[74] *Samtools* v1.17 was then used to select for reads that aligned to the *P. ovale* portion of the dual reference genome rather than that of *P. falciparum*, thus discarding reads from contaminating *P. falciparum* DNA present in some isolates.[75] Resulting alignments of reads that preferentially mapped to *P. ovale* were soft-clipped to reference genome edges and cleaned of unmapped reads using *GATK*, after which mapping proportion and coverage of the ovale reference genome were calculated by *samtools* and *bedtools* v2.30.[76] Additional details about sequencing data processing are available in **Supplemental Methods** and **Data Availability.**

Variant calling from aligned reads across each ovale species genome was also performed using the *GATK* best practices pipeline.[74] In the resulting callset, variants were masked if they fell outside of the 14 chromosomes of the reference genome or were part of specific expanded gene families (see **Supplemental Methods**). *GATK* hard filtering was then used to remove variants with poor quality metrics using the following filter thresholds: quality by depth <3, Fisher strand bias >50, strand odds ratio >3, mapping quality >50, mapping quality rank sum <-2.5, read position rank sum <-3. Callsets were limited to biallelic single nucleotide polymorphisms (SNPs) that were present in at least 80% of individuals. SNP density across the entire genome and within specific functional regions of each genome were calculated using custom scripts (see **Data Availability**). *SNPeff* v4.3 was used to annotate individual variants and determine the ratio of nonsynonymous-to-synonymous mutations.[28,77]

Selection of *P. falciparum* comparison dataset

Co-endemic *P. falciparum* samples were drawn from the Pf6 dataset.[38] Of 20,705 total *P. falciparum* isolates from around the globe, 2,077 came from the same or nearby geographic locations as the source studies of *P. ovale* isolates described above. Thirty-two *P. falciparum* samples with over 85% base callability were randomly selected in order to have at least one co-endemic *P. falciparum* isolate for each *P. ovale curtisi* or *ovale wallikeri* isolate (**Supplemental Table 2**). Variant callsets for these *P. falciparum* samples were limited to the falciparum core genome,[73] quality filtered by Variant Quality Score Recalibration,[74] and restricted to sites present in at least 80% of individuals.

Population genetic analyses

Complexity of infection was estimated for all samples using *THE REAL McCOIL* via the *McCOILR* package.[78] Principal components were calculated and overall genomic similarity compared among monoclonal isolates using *PLINK* v1.90b6.21.[79] Nucleotide diversity was estimated among sets of one-to-one orthologous genes between monoclonal *Poc, Pow*, and *P. falciparum* isolates using *vcftools* v0.1.15.[80] For signatures of selection, nS_L was calculated for all non-missing variants in monoclonal isolates of each *P. ovale* species using *selscan* v1.2.0,[81] while Tajima's D was calculated in 300bp sliding windows in protein-coding genes using *vcf-kit* v0.2.9.[82] Additional details on statistical methodology can be found in the **Supplemental Methods**.

Acknowledgements: We thank all the participants of the parent studies for providing the biological material for the study. The following reagents were obtained through BEI Resources,

NIAID, NIH: 1) *Plasmodium falciparum*, Strain 3D7A, MRA-151, contributed by David Walliker and 2) Diagnostic Plasmid Containing the Small Subunit Ribosomal RNA Gene (18S) from Plasmodium ovale, MRA-180, contributed by Peter A. Zimmerman. We also thank Dr. Parul Johri for her feedback on the final manuscript and Dr. Kevin Wamae for his support in bioinformatic pipeline construction.

Ethics: This analysis was considered non-human subjects research by the University of North Carolina. The appropriate collection of samples and IRBs involved are summarized in the original studies outlined in **Supplemental Table 1**.

Data Availability: All new sequence data are available at NCBI SRA (BioProject ID: PRJNA1092086). Public data used include European Nucleotide Archive Study Accession Number: PRJEB51041 (Run Accession Numbers: ERR10738334, ERR10738339, ERR10738341, ERR10738346), SRA Study Accession Number: PRJEB13344 (Run Accession Numbers: ERR1739852, ERR1739853), SRA Study Accession Number: PRJEB12679 (Run Accession Numbers: ERR1428159, ERR1254542, ERR1254543), SRA Study Accession Numbers: PRJNA1015456 (Run Accession Numbers: SRR26037552, SRR26037551, SRR26037550, SRR26037549, SRR26037548, SRR26037546, SRR26037545, SRR26037544,, SRR26037543, SRR26037542, SRR26037541), and additional Run Accession Numbers: ERR404145, ERR404154, ERR377533, ERR404191, ERR404207, ERR1045266, ERR1045267, ERR676479, ERR1106575, ERR1106579, ERR1106586, ERR1106587, ERR1106590, ERR449901, ERR449903, ERR405238, ERR405244, ERR666939, ERR562889, ERR636018, ERR912913, ERR1514567, ERR1045287, ERR1172616, ERR1172593, ERR1172615, ERR1172608, ERR059405, ERR045598, ERR666937, ERR580480, ERR701763. All code for processing and analysis of samples is available at https://github.com/bailey-lab/Po_popgen_snakemake/tree/main/final. All other data or queries will be made available by the corresponding author on reasonable request.

Author Contributions: KCE, JTL, JJJ and JBP conceived and designed the study. SF, BG, FP, KM, OA, DI, IA, BB, BN, AK, and AT contributed to clinical sample collection. KCE, ZPH, MM, and CG conducted laboratory work. KCE, ZPH, AS, KN, and AS conducted data analysis. KCE drafted the first version of the manuscript. KCE, JTL, JJJ, ZPH, JB, and JP edited and finalized the manuscript.

Competing Interests: J.B.P. reports research support from Gilead Sciences, non-financial support from Abbott Laboratories, and consulting for Zymeron Corporation, all outside the scope of this study. The remaining authors declare no competing interests.

Funding: This study was funded by the National Institute for Allergy and Infectious Diseases, National Institutes of Health (R01AI137395 to JTL, R21AI152260 to JTL, R21AI148579 to JBP and JTL, R01AI65537 to JJJ, K24AI134990 to JJJ, R01AI129812 to AT, R01AI132547 to JJJ, R01TW010870 to JJJ, T32AI070114 supporting KCE), the Fogarty Center, the Global Fund to Fight AIDS, Tuberculosis, and Malaria, and the Bill and Melinda Gates Foundation (Inv. No. 002202 to DI, JJJ and JAB). Under the grant conditions of the Bill and Melinda Gates

Foundation, a Creative Commons Attribution 4.0 Generic License has already been assigned to the Author Accepted Manuscript version that might arise from this submission.

Disclaimer: The findings and conclusions in this report are those of the author(s) and do not necessarily represent the official position of the Bill and Melinda Gates Foundation or other funders.

References

1. Geneva: World Health Organization. *World Malaria Report 2023*. vol. Licence: CC BY-NC-SA 3.0 IGO. (2023).
2. Lover, A. A., Baird, J. K., Gosling, R. & Price, R. N. Malaria Elimination: Time to Target All Species. *Am. J. Trop. Med. Hyg.* **99**, 17–23 (2018).
3. Betson, M., Clifford, S. & Stanton, M. Emergence of Nonfalciparum Plasmodium Infection Despite Regular Artemisinin Combination Therapy in an 18-Month Longitudinal Study of Ugandan Children and …. *The Journal of* (2018).
4. Yman, V. *et al.* Persistent transmission of Plasmodium malariae and Plasmodium ovale species in an area of declining Plasmodium falciparum transmission in eastern Tanzania. *PLoS Negl. Trop. Dis.* **13**, e0007414 (2019).
5. Akala, H. M. *et al.* Plasmodium interspecies interactions during a period of increasing prevalence of Plasmodium ovale in symptomatic individuals seeking treatment: an observational study. *The Lancet Microbe* vol. 2 e141–e150 Preprint at https://doi.org/10.1016/s2666-5247(21)00009-4 (2021).
6. Amato, R. *et al.* Genetic markers associated with dihydroartemisinin–piperaquine failure in Plasmodium falciparum malaria in Cambodia: a genotype–phenotype association study. *Lancet Infect. Dis.* **17**, 164–173 (2017).
7. Bailey, J. A. *et al.* Microarray analyses reveal strain-specific antibody responses to Plasmodium falciparum apical membrane antigen 1 variants following natural infection and vaccination. *Sci. Rep.* **10**, 3952 (2020).

8. Amambua-Ngwa, A. *et al.* Major subpopulations of Plasmodium falciparum in sub-Saharan Africa. *Science* **365**, 813–816 (2019).
9. Volkman, S. K. *et al.* A genome-wide map of diversity in Plasmodium falciparum. *Nat. Genet.* **39**, 113–119 (2007).
10. Ghansah, A. *et al.* Monitoring parasite diversity for malaria elimination in sub-Saharan Africa. *Science* **345**, 1297–1298 (2014).
11. Collins, W. E. & Jeffery, G. M. Plasmodium ovale: parasite and disease. *Clin. Microbiol. Rev.* **18**, 570–581 (2005).
12. Mueller, I., Zimmerman, P. A. & Reeder, J. C. Plasmodium malariae and Plasmodium ovale--the 'bashful'malaria parasites. *Trends Parasitol.* **23**, 278–283 (2007).
13. Calderaro, A. *et al.* Genetic polymorphisms influence Plasmodium ovale PCR detection accuracy. *J. Clin. Microbiol.* **45**, 1624–1627 (2007).
14. Sutherland, C. J. *et al.* Two nonrecombining sympatric forms of the human malaria parasite Plasmodium ovale occur globally. *J. Infect. Dis.* **201**, 1544–1550 (2010).
15. Higgins, M. *et al.* New reference genomes to distinguish the sympatric malaria parasites, Plasmodium ovale curtisi and Plasmodium ovale wallikeri. *Sci. Rep.* **14**, 3843 (2024).
16. Šlapeta, J., Sutherland, C. J. & Fuehrer, H.-P. Calling them names: variants of Plasmodium ovale. *Trends Parasitol.* (2023) doi:10.1016/j.pt.2023.12.010.
17. Snounou, G., Sharp, P. M. & Culleton, R. Appropriate naming of the two Plasmodium ovale species. *Trends Parasitol.* **40**, 207–208 (2024).
18. Snounou, G., Sharp, P. M. & Culleton, R. The two parasite species formerly known as Plasmodium ovale. *Trends Parasitol.* **40**, 21–27 (2024).
19. Oguike, M. C. *et al.* Plasmodium ovale curtisi and Plasmodium ovale wallikeri circulate simultaneously in African communities. *International Journal for Parasitology* vol. 41 677–683 Preprint at https://doi.org/10.1016/j.ijpara.2011.01.004 (2011).
20. Fuehrer, H.-P. *et al.* Plasmodium ovale in Bangladesh: genetic diversity and the first known

evidence of the sympatric distribution of Plasmodium ovale curtisi and Plasmodium ovale wallikeri in southern Asia. *Int. J. Parasitol.* **42**, 693–699 (2012).

21. Fuehrer, H.-P., Campino, S. & Sutherland, C. J. The primate malaria parasites Plasmodium malariae, Plasmodium brasilianum and Plasmodium ovale spp.: genomic insights into distribution, dispersal and host transitions. *Malaria Journal* vol. 21 Preprint at https://doi.org/10.1186/s12936-022-04151-4 (2022).
22. Sendor, R. *et al.* Similar Prevalence of Plasmodium falciparum and Non–P. falciparum Malaria Infections among Schoolchildren, Tanzania. *Emerging Infectious Disease journal* **29**, 1143 (2023).
23. Lei, Y. *et al.* Low genetic diversity and strong immunogenicity within the apical membrane antigen-1 of plasmodium ovale spp. imported from africa to china. *Acta Trop.* **210**, 105591 (2020).
24. Chen, J. *et al.* Disparate selection of mutations in the dihydrofolate reductase gene (dhfr) of Plasmodium ovale curtisi and P. o. wallikeri in Africa. *PLoS Negl. Trop. Dis.* **16**, e0010977 (2022).
25. Joste, V. *et al.* Plasmodium ovale spp dhfr mutations associated with reduced susceptibility to pyrimethamine in sub-Saharan Africa: a retrospective genetic epidemiology and functional study. *Lancet Microbe* **5**, 669–678 (2024).
26. Bright, A. T. *et al.* Whole genome sequencing analysis of Plasmodium vivax using whole genome capture. *BMC Genomics* **13**, 262 (2012).
27. Joste, V., Guillochon, E., Clain, J., Coppée, R. & Houzé, S. Development and Optimization of a Selective Whole-Genome Amplification To Study Plasmodium ovale Spp. *Microbiol Spectr* e0072622 (2022).
28. Rutledge, G. G. *et al.* Plasmodium malariae and P. ovale genomes provide insights into malaria parasite evolution. *Nature* vol. 542 101–104 Preprint at https://doi.org/10.1038/nature21038 (2017).

29. Feleke, S. M. *et al.* Plasmodium falciparum is evolving to escape malaria rapid diagnostic tests in Ethiopia. *Nat Microbiol* **6**, 1289–1299 (2021).
30. Parr, J. B. *et al.* Analysis of false-negative rapid diagnostic tests for symptomatic malaria in the Democratic Republic of the Congo. *Sci. Rep.* **11**, 6495 (2021).
31. Mwandagalirwa, M. K. *et al.* Individual and household characteristics of persons with Plasmodium falciparum malaria in sites with varying endemicities in Kinshasa Province, Democratic Republic of the Congo. *Malar. J.* **16**, 456 (2017).
32. Tarimo, B. B. *et al.* Seasonality and transmissibility of Plasmodium ovale in Bagamoyo District, Tanzania. *Parasit. Vectors* **15**, 56 (2022).
33. Rogier, E. *et al.* Plasmodium falciparum pfhrp2 and pfhrp3 gene deletions among patients enrolled at 100 health facilities throughout Tanzania: February to July 2021. *bioRxiv* (2023) doi:10.1101/2023.07.29.23293322.
34. Ali, I. M. *et al.* Arboviruses as an unappreciated cause of non-malarial acute febrile illness in the Dschang Health District of western Cameroon. *PLoS Negl. Trop. Dis.* **16**, e0010790 (2022).
35. Venkatesan, M. *et al.* Using CF11 cellulose columns to inexpensively and effectively remove human DNA from Plasmodium falciparum-infected whole blood samples. *Malar. J.* **11**, 41 (2012).
36. Joste, V. *et al.* Genetic Profiling of Plasmodium ovale wallikeri Relapses With Microsatellite Markers and Whole-Genome Sequencing. *J. Infect. Dis.* **228**, 1089–1098 (2023).
37. Ansari, H. R. *et al.* Genome-scale comparison of expanded gene families in Plasmodium ovale wallikeri and Plasmodium ovale curtisi with Plasmodium malariae and with other Plasmodium species. *Int. J. Parasitol.* **46**, 685–696 (2016).
38. MalariaGEN *et al.* An open dataset of Plasmodium falciparum genome variation in 7,000 worldwide samples. *Wellcome Open Res.* **6**, 42 (2021).
39. Sendor, R. *et al.* Epidemiology of Plasmodium malariae and Plasmodium ovale spp. in

Kinshasa Province, Democratic Republic of Congo. *Nat. Commun.* **14**, 6618 (2023).

40. Bright, A. T. *et al.* A high resolution case study of a patient with recurrent Plasmodium vivax infections shows that relapses were caused by meiotic siblings. *PLoS Negl. Trop. Dis.* **8**, e2882 (2014).
41. Sirawaraporn, W., Sathitkul, T., Sirawaraporn, R., Yuthavong, Y. & Santi, D. V. Antifolate-resistant mutants of Plasmodium falciparum dihydrofolate reductase. *Proc. Natl. Acad. Sci. U. S. A.* **94**, 1124–1129 (1997).
42. Hastings, M. D. *et al.* Dihydrofolate reductase mutations in Plasmodium vivax from Indonesia and therapeutic response to sulfadoxine plus pyrimethamine. *J. Infect. Dis.* **189**, 744–750 (2004).
43. Ferrer-Admetlla, A., Liang, M., Korneliussen, T. & Nielsen, R. On detecting incomplete soft or hard selective sweeps using haplotype structure. *Mol. Biol. Evol.* **31**, 1275–1291 (2014).
44. Gomes, A. R. *et al.* A transcriptional switch controls sex determination in Plasmodium falciparum. *Nature* **612**, 528–533 (2022).
45. Russell, A. J. C. *et al.* Regulators of male and female sexual development are critical for the transmission of a malaria parasite. *Cell Host Microbe* **31**, 305–319.e10 (2023).
46. Tadesse, F. G. *et al.* Gametocyte Sex Ratio: The Key to Understanding Plasmodium falciparum Transmission? *Trends Parasitol.* **35**, 226–238 (2019).
47. Khan, S. M. *et al.* Proteome analysis of separated male and female gametocytes reveals novel sex-specific Plasmodium biology. *Cell* **121**, 675–687 (2005).
48. Douradinha, B. *et al.* Plasmodium Cysteine Repeat Modular Proteins 3 and 4 are essential for malaria parasite transmission from the mosquito to the host. *Malar. J.* **10**, 71 (2011).
49. Thompson, J. *et al.* Plasmodium cysteine repeat modular proteins 1-4: complex proteins with roles throughout the malaria parasite life cycle. *Cell. Microbiol.* **9**, 1466–1480 (2007).
50. Lyons, F. M. T., Gabriela, M., Tham, W.-H. & Dietrich, M. H. Plasmodium 6-cysteine proteins: Functional diversity, transmission-blocking antibodies and structural scaffolds.

Front. Cell. Infect. Microbiol. **12**, 945924 (2022).

51. Arumugam, T. U. *et al.* Discovery of GAMA, a Plasmodium falciparum merozoite micronemal protein, as a novel blood-stage vaccine candidate antigen. *Infect. Immun.* **79**, 4523–4532 (2011).
52. Patarroyo, M. E., Alba, M. P. & Curtidor, H. Biological and structural characteristics of the binding peptides from the sporozoite proteins essential for cell traversal (SPECT)-1 and -2. *Peptides* **32**, 154–160 (2011).
53. Tebben, K. *et al.* Malian children infected with Plasmodium ovale and Plasmodium falciparum display very similar gene expression profiles. *PLoS Negl. Trop. Dis.* **17**, e0010802 (2023).
54. Tajima, F. Statistical method for testing the neutral mutation hypothesis by DNA polymorphism. *Genetics* **123**, 585–595 (1989).
55. Singh, G. P. & Sharma, A. South-East Asian strains of Plasmodium falciparum display higher ratio of non-synonymous to synonymous polymorphisms compared to African strains. *F1000Res.* **5**, 1964 (2016).
56. Feng, X. *et al.* Single-nucleotide polymorphisms and genome diversity in Plasmodium vivax. *Proc. Natl. Acad. Sci. U. S. A.* **100**, 8502–8507 (2003).
57. Chang, H.-H. *et al.* Malaria life cycle intensifies both natural selection and random genetic drift. *Proc. Natl. Acad. Sci. U. S. A.* **110**, 20129–20134 (2013).
58. Saralamba, N. *et al.* Genetic dissociation of three antigenic genes in Plasmodium ovale curtisi and Plasmodium ovale wallikeri. *PLoS One* **14**, e0217795 (2019).
59. Faye, F. B. K. *et al.* Diagnostic criteria and risk factors for Plasmodium ovale malaria. *J. Infect. Dis.* **186**, 690–695 (2002).
60. Thomson-Luque, R., Stabler, T. C., Fürle, K., Silva, J. C. & Daubenberger, C. Plasmodium falciparum merozoite surface protein 1 as asexual blood stage malaria vaccine candidate. *Expert Rev. Vaccines* **23**, 160–173 (2024).

61. Escalante, A. A., Lal, A. A. & Ayala, F. J. Genetic polymorphism and natural selection in the malaria parasite Plasmodium falciparum. *Genetics* **149**, 189–202 (1998).
62. Chu, R. *et al.* Limited genetic diversity of N-terminal of merozoite surface protein-1 (MSP-1) in Plasmodium ovale curtisi and P. ovale wallikeri imported from Africa to China. *Parasit. Vectors* **11**, 596 (2018).
63. Joyner, C. J. *et al.* Humoral immunity prevents clinical malaria during Plasmodium relapses without eliminating gametocytes. *PLoS Pathog.* **15**, e1007974 (2019).
64. Thiam, L. G., Mangou, K., Ba, A., Mbengue, A. & Bei, A. K. Leveraging genome editing to functionally evaluate Plasmodium diversity. *Trends Parasitol.* **38**, 558–571 (2022).
65. Mohring, F. *et al.* Cation ATPase (ATP4) orthologue replacement in the malaria parasite Plasmodium knowlesi reveals species-specific responses to ATP4-targeting drugs. *MBio* **13**, e0117822 (2022).
66. Siegel, S. V. *et al.* Lineage-informative microhaplotypes for recurrence classification and spatio-temporal surveillance of Plasmodium vivax malaria parasites. *Nat. Commun.* **15**, 6757 (2024).
67. Liu, P. *et al.* Increasing proportions of relapsing parasite species among imported malaria in China's Guangxi Province from Western and Central Africa. *Travel Med. Infect. Dis.* **43**, 102130 (2021).
68. Wångdahl, A. *et al.* Relapse of Plasmodium vivax and Plasmodium ovale Malaria With and Without Primaquine Treatment in a Nonendemic Area. *Clin. Infect. Dis.* **74**, 1199–1207 (2022).
69. Potlapalli, V. R. *et al.* Real-time PCR detection of mixed Plasmodium ovale curtisi and wallikeri infections in human and mosquito hosts. *PLoS Negl. Trop. Dis.* **17**, e0011274 (2023).
70. Mitchell, C. L. *et al.* Under the Radar: Epidemiology of Plasmodium ovale in the Democratic Republic of the Congo. *J. Infect. Dis.* **223**, 1005–1014 (2021).

71. Clarke, E. L. *et al.* swga: a primer design toolkit for selective whole genome amplification. *Bioinformatics* **33**, 2071–2077 (2017).
72. Mölder, F. *et al.* Sustainable data analysis with Snakemake. *F1000Res.* **10**, 33 (2021).
73. Miles, A. *et al.* Indels, structural variation, and recombination drive genomic diversity in Plasmodium falciparum. *Genome Res.* **26**, 1288–1299 (2016).
74. Van der Auwera, G. A. & O'Connor, B. D. *Genomics in the Cloud: Using Docker, GATK, and WDL in Terra*. ('O'Reilly Media, Inc.', 2020).
75. Li, H. *et al.* The Sequence Alignment/Map format and SAMtools. *Bioinformatics* **25**, 2078–2079 (2009).
76. Quinlan, A. R. & Hall, I. M. BEDTools: a flexible suite of utilities for comparing genomic features. *Bioinformatics* **26**, 841–842 (2010).
77. Cingolani, P. *et al.* A program for annotating and predicting the effects of single nucleotide polymorphisms, SnpEff: SNPs in the genome of Drosophila melanogaster strain w1118; iso-2; iso-3. *Fly* **6**, 80–92 (2012).
78. Chang, H.-H. *et al.* THE REAL McCOIL: A method for the concurrent estimation of the complexity of infection and SNP allele frequency for malaria parasites. *PLoS Comput. Biol.* **13**, e1005348 (2017).
79. Purcell, S. *et al.* PLINK: a tool set for whole-genome association and population-based linkage analyses. *Am. J. Hum. Genet.* **81**, 559–575 (2007).
80. Danecek, P. *et al.* The variant call format and VCFtools. *Bioinformatics* **27**, 2156–2158 (2011).
81. Szpiech, Z. A. & Hernandez, R. D. selscan: An Efficient Multithreaded Program to Perform EHH-Based Scans for Positive Selection. *Molecular Biology and Evolution* vol. 31 2824–2827 Preprint at https://doi.org/10.1093/molbev/msu211 (2014).
82. Cook, D. E. & Andersen, E. C. VCF-kit: assorted utilities for the variant call format. *Bioinformatics* **33**, 1581–1582 (2017).